TABLE III. Results of Multivariate Logistic Analysis for Factors Associated With the High AFP Levels at the Initial Visit

Factor	Category	Risk ratio (95%CI)	P
Patients with the HBsAg levels above 500 IU/ml (n = 1,277)			
HBsAg (IU/ml)	1: ≥7,000	1	
	2: <7,000	3.69 (2.12–6.41)	<0.001
Albumin (g/dl)	1: ≥3.9	1	
	2: <3.9	3.09 (1.88–5.05)	<0.001
Platelet count ($\times 10^4$/mm^3)	1: ≥20.0	1	
	2: <20.0	2.50 (1.47–4.24)	0.001
Gamma-glutamyl transpeptidase (IU/L)	1: <50	1	
	2: ≥50	2.28 (1.40–3.72)	0.001
Aspartate aminotransferase (IU/L)	1: <34	1	
	2: ≥34	2.77 (1.42–5.39)	0.003
HBeAg	1: Negative	1	
	2: Positive	2.07 (1.24–3.45)	0.005
HBcrAg (log U/ml)	1: <3.0	1	
	2: ≥3.0	5.10 (1.16–22.4)	0.031
Patients with the HBsAg levels below 500 IU/ml (n = 333)			
Albumin (g/dl)	1: ≥3.9	1	
	2: <3.9	12.8 (4.02–41.7)	<0.001
Gamma-glutamyl transpeptidase (IU/L)	1: <50	1	
	2: ≥50	6.95 (2.06–23.5)	0.002
HBcrAg (log U/ml)	1: <3.0	1	
	2: ≥3.0	5.62 (1.51–21.0)	0.010

Low transaminase levels were defined as transaminase levels below the upper limit of normal.

had low transaminase levels (AST ≤33 IU/L and ALT ≤42 IU/L, i.e., below the upper limits of normal) to further determine those factors that determine the high level of AFP at the initial visit. High AFP was detected in 26 (6.1%) patients among 426 with the HBsAg levels above 500 IU/ml and low transaminase levels. Using the data of these patients, univariate analysis identified three parameters that correlated significantly with a high AFP level at the initial visit. These included albumin (<3.9 g/dl; $P = 0.004$), platelet count (<20.0 × 10^4/mm^3; $P = 0.012$), and HBsAg levels (<7,000 IU/ml; $P = 0.004$). Multivariate analysis that included the above variables identified albumin (<3.9 g/dl; OR 3.92, $P = 0.001$) and HBsAg levels (<7,000 IU/ml; OR 4.33, $P = 0.004$) as independent determinants of a high AFP level at the initial visit (Table IV).

Among 192 patients with the HBsAg levels below 500 IU/ml and low transaminase levels, high AFP levels were detected at the initial visit in 12 (6.3%). Univariate analysis identified three parameters that influenced significantly the elevated AFP level at the initial visit. These included albumin (<3.9 g/dl; $P = 0.010$), GGT (≥50 IU/L; $P = 0.011$), and platelet count (<20.0 × 10^4/mm^3; $P = 0.020$). Multivariate analysis that included these variables identified albumin (<3.9 g/dl; OR 7.19, $P = 0.004$) as the only independent determinant of a high AFP level at the initial visit (Table IV).

TABLE IV. Results of Multivariate Analysis for Factors Associated With the High AFP Levels at the Initial Visit

Factor	Category	Risk ratio (95%CI)	P
Patients with HBsAg >500 IU/ml and low transaminase levels (n = 426)			
Albumin (g/dl)	1: ≥3.9	1	
	2: <3.9	3.92 (1.71–9.01)	0.001
HBsAg (IU/ml)	1: ≥7,000	1	
	2: <7,000	4.33 (1.58–11.9)	0.004
Patients with HBsAg <500 IU/ml and low transaminase levels (n = 192)			
Albumin (g/dl)	1: ≥3.9	1	
	2: <3.9	7.19 (1.87–27.8)	0.004

Low transaminase levels were defined as transaminase levels below the upper limit of normal.

DISCUSSION

There is little information on the cutoff value of AFP that can be used to predict the future probability of HCC in patients with HBV infection. The present study followed-up patients naïve to antiviral therapy from the initial visit and showed that the rate of hepatocarcinogenesis was significantly higher in those with high AFP levels at the baseline than those with low levels. To our knowledge, the present study is the first to report the hepatocarcinogenesis rate stratified according to the AFP level in patients infected with HBV but free of HCC at the initial visit, based on a large-scale long-term follow-up cohort. The results indicated that patients with high AFP levels at the initial visit are at high risk of HCC, and emphasize the need to determine the factors that could affect the AFP level as surrogate markers of early hepatocarcinogenesis. Previous studies in patients with HCV infection indicated that suppression of the AFP level by treatment with interferon reduced the HCC risk even in those without complete eradication of HCV [Arase et al., 2007; Asahina et al., 2013]. However, there is little

evidence that suppression of the AFP level by antiviral therapy reduces the HCC risk in patients with HBV infection. Further prospective studies are needed to investigate this issue in detail.

In the present study, the relationship between the HBsAg levels and the AFP levels detected at the initial visit suggested the presence of two distinct groups within the study patients. Interestingly, in patients with the HBsAg levels above 500 IU/ml, a significant negative correlation was observed between the HBsAg and the AFP levels, and a significant positive correlation was observed between the HBsAg and the platelet count. Previous studies indicated that high serum AFP levels correlated with liver fibrosis Stage 3 and 4 [Bayati et al., 1998; Chu et al., 2001; Hu et al., 2002, 2004], and that lower thrombocytopenia was closely associated with advanced liver disease [Ikeda et al., 2009; Akuta et al., 2012]. Considered together, these results emphasize the importance of hyper-α-fetoproteinemia and thrombocytopenia in the prediction of severe liver fibrosis, respectively. Based on the present results and the recent reports suggesting the potential correlation between the HBsAg level and the stage of liver fibrosis [Seto et al., 2012; Martinot-Peignoux et al., 2013], it is possible that HBsAg levels could correlate with the stage of fibrosis in patients with the HBsAg levels above 500 IU/ml. Further studies are needed to determine the value of hyper-α-fetoproteinemia in patients with low and high HBsAgemia.

In addition to the HBsAg level, multivariate analysis also identified HBcrAg as another viral factor that influenced independently the AFP level at the baseline. HBcrAg comprises HBcAg, HBeAg and a 22-kDa precore protein coded with the precore/core gene [Kimura et al., 2002, 2005]. Previous studies reported a significant correlation between serum HBcrAg concentrations and intrahepatic levels of covalently closed circular DNA (cccDNA) [Wong et al., 2007; Suzuki et al., 2009]. Other studies indicated that HBcrAg is a useful predictor of HCC during antiviral therapy [Kumada et al., 2013], and post-treatment recurrence of HCC during antiviral therapy [Hosaka et al., 2010]. The present study, based on patients naïve to antiviral therapy showed that high serum HBcrAg concentrations also correlated with high AFP at the initial visit. This is the first report demonstrating the potential usefulness of HBcrAg as a surrogate marker for early hepatocarcinogenesis.

The impact of the HBsAg level on hepatocarcinogenesis is not clear at this stage. In this study, the effect of the HBsAg levels at the initial visit on HCC was assessed in 1,061 consecutive antiviral therapy-naive patients infected with HBV. Analysis of data of 794 patients with the HBsAg levels above 500 IU/ml at the initial visit (after exclusion of patients on antiviral therapy) showed a significantly lower cumulative HCC rate in patients with the HBsAg levels above 7,000 IU/ml than those with levels below 7,000 IU/ml ($P < 0.001$, Log-rank test, Fig. 4). This result suggests that HBsAg levels at the baseline do not only influence AFP, but also play a role in hepatocarcinogenesis. Further studies need to be performed to determine the pathomechanisms of HBsAg in hepatocarcinogenesis.

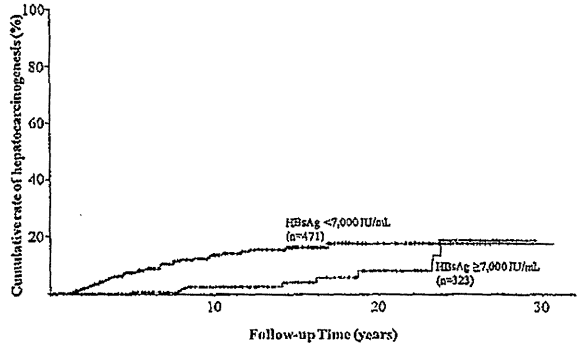

Fig. 4. Cumulative rate of hepatocarcinogenesis stratified according to the HBsAg levels at the initial visit in patients naïve to antiviral therapy from the initial visit until last visit. In a preliminary study based on 794 patients with the HBsAg levels above 500 IU/ml at the initial visit, the cumulative hepatocarcinogenesis rate for patients with the HBsAg levels more than 7,000 IU/ml was significantly lower than for those with levels below 7,000 IU/ml ($P < 0.001$; Log-rank test).

The present study has certain limitations. First, the study did not examine the effects of other genotypes, apart from HBV genotype B or C. Second, the study population was limited to Japanese and did not include other races, and thus generalization of the results to other races cannot be made based on the results. Third, the study did not investigate the effects of antiviral therapy (interferon and/or nucleot(s)ide analogs) on the outcome since such therapy suppressed the AFP levels and thus reduce the risk of HCC in patients with HBV infection.

In conclusion, the present studies demonstrated that the HBsAg level seem to influence the AFP levels and can be used as a surrogate marker for early hepatocarcinogenesis in patients with hepatitis B viral infection.

REFERENCES

Akuta N, Suzuki F, Seko Y, Kawamura Y, Sezaki H, Suzuki Y, Hosaka T, Kobayashi M, Hara T, Kobayashi M, Saitoh S, Arase Y, Ikeda K, Kumada H. 2012. Complicated relationships of amino acid substitution in hepatitis C virus core region and IL28B genotype influencing hepatocarcinogenesis. Hepatology 56:2134–2141.

Alpert E, Feller ER. 1978. α-fetoprotein (AF) in benign liver disease. Gastroenterology 74:856–858.

Arase Y, Ikeda K, Suzuki F, Suzuki Y, Kobayashi M, Akuta N, Hosaka T, Sezaki H, Yatsuji H, Kawamura Y, Kobayashi M, Kumada H. 2007. Prolonged-interferon therapy reduces hepatocarcinogenesis in aged-patients with chronic hepatitis C. J Med Virol 79:1095–1102.

Asahina Y, Tsuchiya K, Nishimura T, Muraoka M, Suzuki Y, Tamaki N, Yasui Y, Hosokawa T, Ueda K, Nakanishi H, Itakura J, Takahashi Y, Kurosaki M, Enomoto N, Nakagawa M, Kakinuma S, Watanabe M, Izumi N. 2013. α-Fetoprotein levels after interferon therapy and risk of hepatocarcinogenesis in chronic hepatitis C. Hepatology 58:1253–1262.

Bayati N, Silverman Al, Gordon SC. 1998. Serum alpha-fetoprotein levels and liver histology in patients with chronic hepatitis C. Am J Gastroenterol 93:2452–2456.

Bergstrand CG, Czar B. 1956. Demonstration of a new protein fraction in serum from the human fetus. Scand J Clin Lab Invest 8:174.

Bruix J, Sherman M. 2005. Practice guidelines committee, American Association for the Study of Liver Diseases. Management of hepatocellular carcinoma. Hepatology 42:1208–1236.

Brunetto MR, Moriconi F, Bonino F, Lau GK, Farci P, Yurdaydin C, Piratvisuth T, Luo K, Wang Y, Hadziyannis S, Wolf E, McCloud P, Batrla R, Marcellin P. 2009. Hepatitis B virus surface antigen levels: A guide to sustained response to peginterferon alfa-2a in HBeAg-negative chronic hepatitis B. Hepatology 49:1141–1150.

Brunetto MR, Oliveri F, Colombatto P, Moriconi F, Ciccorossi P, Coco B, Romagnoli V, Cherubini B, Moscato G, Maina AM, Cavallone D, Bonino F. 2010. Hepatitis B surface antigen serum levels help to distinguish active from inactive hepatitis B virus genotype D carriers. Gastroenterology 139:483–490.

Chan HL. 2012. Identifying hepatitis B carriers at low risk for hepatocellular carcinoma. Gastroenterology 142:1057–1060.

Chan HL, Wong VW, Wong GL, Tse CH, Chan HY, Sung JJ. 2010. A longitudinal study on the natural history of serum hepatitis B surface antigen changes in chronic hepatitis B. Hepatology 52:1232–1241.

Chan HL, Thompson A, Martinot-Peignoux M, Piratvisuth T, Cornberg M, Brunetto MR, Tillmann HL, Kao JH, Jia JD, Wedemeyer H, Locarnini S, Janssen HL, Marcellin P. 2011. Hepatitis B surface antigen quantification: Why and how to use it in 2011—A core group report. J Hepatol 55:1121–1131.

Cheema AW, Hirschtritt T, Van Thiel DH. 2004. Markedly elevated alpha-fetoprotein levels without hepatocellular carcinoma. Hepatogastroenterology 51:1676–1678.

Chen DS, Sung JL. 1979. Relationship of hepatitis B surface antigen to serum alpha-fetoprotein in nonmalignant diseases of the liver. Cancer 44:984–992.

Chu CW, Hwang SJ, Luo JC, Lai CR, Tsay SH, Li CP, Wu JC, Chang FY, Lee SD. 2001. Clinical, virological, and pathologic significance of elevated serum alpha-fetoprotein levels in patients with chronic hepatitis C. J Clin Gastroenterol 32:240–244.

Di Bisceglie AM, Hoofnagle JH. 1989. Elevations in serum alpha-fetoprotein levels in patients with chronic hepatitis B. Cancer 64:2117–2120.

Ebara M, Ohto M, Shinagawa T, Sugiura N, Kimura K, Matsutani S, Morita M, Saisho H, Tsuchiya Y, Okuda K. 1986. Natural history of minute hepatocellular carcinoma smaller than three centimeters complicating cirrhosis. A study in 22 patients. Gastroenterology 90:289–298.

Elftherious N, Heathcote J, Thomas HC, Sherlock S. 1977. Serum alpha-fetoprotein levels in patients with acute and chronic liver disease. J Clin Pathol 30:704–708.

Hosaka T, Suzuki F, Kobayashi M, Hirakawa M, Kawamura Y, Yatsuji H, Sezaki H, Akuta N, Suzuki Y, Saitoh S, Arase Y, Ikeda K, Kobayashi M, Kumada H. 2010. HBcrAg is a predictor of post-treatment recurrence of hepatocellular carcinoma during antiviral therapy. Liver Int 30:1461–1470.

Hu KQ, Esrailian E, Thompson K, Chase R, Kyulo N, Hassen M, Abdelhalim F, Hillebrand DJ, Runyon BA. 2002. Hepatic steatosis is associated with disease progression of chronic hepatitis C: A large cohort study in the United States. Hepatology 36:349A.

Hu KQ, Kyulo N, Lim N, Elhazin B, Hillebrand DJ, Bock T. 2004. Clinical significance of elevated alpha-fetoprotein (AFP) in patients with chronic hepatitis C, but not hepatocellular carcinoma. Am J Gastroenterol 99:860–865.

Ikeda K, Arase Y, Kawamura Y, Yatsuji H, Sezaki H, Hosaka T, Akuta N, Kobayashi M, Saitoh S, Suzuki F, Suzuki Y, Kumada H. 2009. Necessities of interferon therapy in elderly patients with chronic hepatitis C. Am J Med 122:479–486.

Jaroszewicz J, Calle Serrano B, Wursthorn K, Deterding K, Schlue J, Raupach R, Flisiak R, Bock CT, Manns MP, Wedemeyer H, Cornberg M. 2010. Hepatitis B surface antigen (HBsAg) levels in the natural history of hepatitis B virus (HBV)-infection: A European perspective. J Hepatol 52:514–522.

Johnson PJ. 2001. The role of serum alpha-fetoprotein estimation in the diagnosis and management of hepatocellular carcinoma. Clin Liv Dis 5:145–159.

Kew MC, Purves LR, Bersohn I. 1973. Serum alpha-fetoprotein levels in acute viral hepatitis. Gut 14:939–942.

Kimura T, Rokuhara A, Sakamoto Y, Yagi S, Tanaka E, Kiyosawa K, Maki N. 2002. Sensitive enzyme immunoassay for hepatitis B virus core-related antigens and their correlation to virus load. J Clin Microbiol 40:439–445.

Kimura T, Ohno N, Terada N, Rokuhara A, Matsumoto A, Yagi S, Tanaka E, Kiyosawa K, Ohno S, Maki N. 2005. Hepatitis B virus DNA-negative dane particles lack core protein but contain a 22-kDa precore protein without C-terminal arginine-rich domain. J Biol Chem 280:21713–21719.

Kobayashi M, Arase Y, Ikeda K, Tsubota A, Suzuki Y, Saitoh S, Kobayashi M, Suzuki F, Akuta N, Someya T, Matsuda M, Sato J, Kumada H. 2002. Clinical characteristics of patients infected with hepatitis B virus genotypes A, B, and C. J Gastroenterol 37:35–39.

Kumada T, Toyoda H, Tada T, Kiriyama S, Tanikawa M, Hisanaga Y, Kanamori A, Niinomi T, Yasuda S, Andou Y, Yamamoto K, Tanaka J. 2013. Effect of nucleos(t)ide analogue therapy on hepatocarcinogenesis in chronic hepatitis B patients: A propensity score analysis. J Hepatol 58:427–433.

Liaw YF. 2011. Clinical utility of hepatitis B surface antigen quantitation in patients with chronic hepatitis B: A review. Hepatology 54:E1–E9.

Martinot-Peignoux M, Lada O, Cardoso AC, Lapalus M, Boyer N, Ripault MP, Asselah T, Marcellin P. 2010. Quantitative HBsAg: A new specific marker for the diagnosis of HBsAg inactive carriage. Hepatology 52:992A.

Martinot-Peignoux M, Carvalho-Filho R, Lapalus M, Netto-Cardoso AC, Lada O, Batrla R, Krause F, Asselah T, Marcellin P. 2013. Hepatitis B surface antigen serum level is associated with fibrosis severity in treatment-naïve, E antigen-positive patients. J Hepatol 58:1089–1095.

Moucari R, Mackiewicz V, Lada O, Ripault MP, Castelnau C, Martinot-Peignoux M, Dauvergne A, Asselah T, Boyer N, Bedossa P, Valla D, Vidaud M, Nicolas-Chanoine MH, Marcellin P. 2009. Early serum HBsAg drop: A strong predictor of sustained virological response to pegylated interferon alfa-2a in HBeAg-negative patients. Hepatology 49:1151–1157.

Nguyen T, Thompson AJ, Bowden S, Croagh C, Bell S, Desmond PV, Levy M, Locarnini SA. 2010. Hepatitis B surface antigen levels during the natural history of chronic hepatitis B: A perspective on Asia. J Hepatol 52:508–513.

Sato Y, Nakata K, Kato Y, Shima M, Ishii N, Koji T, Taketa K, Endo Y, Nagataki S. 1993. Early recognition of hepatocellular carcinoma based on altered profiles of alpha-fetoprotein. N Engl J Med 328:1802–1806.

Seto WK, Wong DK, Fung J, Ip PP, Yuen JC, Hung IF, Lai CL, Yuen MF. 2012. High hepatitis B surface antigen levels predict insignificant fibrosis in hepatitis B e antigen positive chronic hepatitis B. PLoS ONE 7:e43087.

Shinagawa T, Ohto M, Kimura K, Tsunetomi S, Morita M, Saisho H, Tsuchiya Y, Saotome N, Karasawa E, Miki M. 1984. Diagnosis and clinical features of small hepatocellular carcinoma with emphasis on the utility of real-time ultrasonography. A study in 51 patients. Gastroenterology 86:495–502.

Silver HK, Gold P, Shuster J, Javitt NB, Freedman SO, Finlayson ND. 1974. Alpha 1-fetoprotein in chronic liver disease. N Engl J Med 291:506–508.

Suzuki F, Miyakoshi H, Kobayashi M, Kumada H. 2009. Correlation between serum hepatitis B virus core-related antigen and intrahepatic covalently closed circular DNA in chronic hepatitis B patients. J Med Virol 81:27–33.

Tseng TC, Liu CJ, Yang HC, Su TH, Wang CC, Chen CL, Kuo SF, Liu CH, Chen PJ, Chen DS, Kao JH. 2012. High levels of hepatitis B surface antigen increase risk of hepatocellular carcinoma in patients with low HBV load. Gastroenterology 142:1140–1149.

Viola LA, Barrison IG, Coleman JC, Paradinas FJ, Fluker JL, Evans BA, Murray-Lyon IM. 1981. Natural history of liver disease in chronic hepatitis B surface antigen carriers. Survey of 100 patients from Great Britain. Lancet 2:1156–1159.

Wong DK, Tanaka Y, Lai CL, Mizokami M, Fung J, Yuen MF. 2007. Hepatitis B virus core-related antigens as markers for monitoring chronic hepatitis B infection. J Clin Microbiol 45:3942–3947.

Yao FY. 2003. Dramatic reduction of the alpha-fetoprotein level after lamivudine treatment of patients with chronic hepatitis B virus infection and cirrhosis. J Clin Gastroenterol 36:440–442.

Hepatology Research

Hepatology Research 2014; 44: 1234–1240 doi: 10.1111/hepr.12240

Short Communication

Potential of a no-touch pincer ablation procedure for small hepatocellular carcinoma that uses a multipolar radiofrequency ablation system: An experimental animal study

Yusuke Kawamura,[1,2] Kenji Ikeda,[1,2] Taito Fukushima,[1,2] Tasuku Hara,[1,2] Tetsuya Hosaka,[1,2] Masahiro Kobayashi,[1,2] Satoshi Saitoh,[1,2] Hitomi Sezaki,[1,2] Norio Akuta,[1,2] Fumitaka Suzuki,[1,2] Yoshiyuki Suzuki,[1,2] Yasuji Arase[1,2] and Hiromitsu Kumada[1,2]

[1]*Department of Hepatology,* [2]*Okinaka Memorial Institute for Medical Research, Toranomon Hospital, Tokyo, Japan*

Aim: Treatment of hepatocellular carcinoma located on the liver surface is frequently difficult because direct puncture of the tumor must be avoided during needle insertion. The aim of this study was to investigate the utility of a no-touch pincer ablation procedure that uses a multipolar radiofrequency ablation (RFA) system for a tumor located on the liver surface.

Methods: The experimental animals were three pigs, and RFA was performed with two internally cooled bipolar electrodes. Three ablative procedures were compared: linear insertion at regular 13-mm intervals (pattern 1; virtual target tumor size, <10 mm); fan-shape insertion, maximum interval 20 mm (pattern 2; virtual target tumor size, <15 mm); and 25 mm (pattern 3; virtual target tumor size, <20 mm). All electrodes were inserted at a 30-mm depth. For patterns 1 and 2, ablation was performed on three other parts of the liver, and for pattern 3, ablation was performed on two other parts.

Results: For the median transverse and longitudinal diameter to the shaft, with the pattern 1 procedure, the ablative areas were 32 mm × 30 mm, and with the pattern 2 procedure, the ablative areas were 27 mm × 30 mm with carbonization of the liver surface. In contrast, with the pattern 3 procedure, the ablative areas were 45 mm × 26 mm; however, the ablative margin did not reach the surface, and carbonization was not apparent.

Conclusion: The no-touch pincer ablation procedure (with an electrode interval of ≤20 mm) may be useful when performed with two internally cooled bipolar electrodes for small nodules that protrude from the liver surface.

Key words: bipolar, hepatocellular carcinoma, multipolar, no-touch ablation, radiofrequency ablation

INTRODUCTION

AMONG THE AVAILABLE treatment options for hepatocellular carcinoma (HCC), surgical resection is generally considered to be a local eradication method that can provide a satisfactory long-term outcome.[1–8] Recent advances in imaging procedures have led to increased detection of early-stage HCC and to improved survival due to the increased identification of patients in whom hepatic resection is possible.[9,10]

For patients who are not eligible for surgery for various reasons (e.g. lack of sufficient liver function for surgical resection), percutaneous local therapy is a viable therapeutic option. Several local ablation therapies are available, including percutaneous ethanol injection, percutaneous acetic acid injection, cryotherapy, percutaneous microwave coagulation therapy and radiofrequency ablation (RFA). In addition to surgical resection, local ablation therapies, particularly RFA, are considered to be local eradication methods for HCC that can provide good long-term outcomes.[11] Therefore, in recent years, RFA has become a widely used option for the primary treatment of small-size HCC. However, we often

Correspondence: Dr Yusuke Kawamura, Department of Hepatology, Toranomon Hospital, 2-2-2 Toranomon, Minato-ku, Tokyo 105-8470, Japan. Email: k-yusuke@toranomon.gr.jp

Funding: Okinaka Memorial Institute for Medical Research and Japanese Ministry of Health, Labor and Welfare.

Conflict of interest: The authors state that they have no conflicts of interest regarding the content of the article.

Author contribution: All authors had access to the data and played a role in writing this manuscript.

Received 29 May 2013; revision 26 August 2013; accepted 10 September 2013.

encounter cases of HCC that are difficult to treat with RFA as a result of tumor location, especially nodules that protrude from the liver surface. In addition, a relationship between percutaneous local approaches to HCC (including tumor biopsy) and tumor seeding has been reported previously,[12,13] and with regard to the risk of treatment-related tumor seeding, the following risk factors have been reported: tumor size, tumor location (subcapsular portion), α-fetoprotein level, tumor stage and histopathological grade.[14,15] Therefore, a no-touch approach to local therapy may be considered an ideal treatment method for HCC.

Recently, a multipolar ablation system became available. Until now, in Japan, monopolar electrodes have typically been used, and the present cases are usually treated with some technical arrangement. For example, in the case of using a multi-tined expandable electrode, after obliquely inserting the electrode to avoid direct puncture of the target tumor, the multi needles are expanded toward the target tumor via non-tumor tissue, or in the case of using an internally cooled electrode, multiple insertions are made to avoid direct puncture of the target tumor, and RFA is performed after each insertion. However, these methods do not always provide enough of a treatment effect due to the influence of uncertain treatment procedures and natural, direct puncture to a tumor is indispensable. In contrast, a multipolar ablation system that uses an internally cooled bipolar electrode can combine the use of one to three electrodes at the same treatment session. When three electrodes are used, this system can treat large tumors; however, in the case of small tumors, it is not really necessary to use three electrodes to treat the target tumor. In addition, when we used this multipolar ablation system, usually electrodes were inserted into HCC, but in theory, this system can use no-touch ablation. However, to our knowledge, there are no technical reports that describe a non-direct punctual RFA method that uses a bipolar ablation system for HCC located on the liver surface. In this experimental animal study, we assumed that a small (<20 mm) HCC nodule protruded from the liver surface, and examined proper pincer ablation methods using two internally cooled bipolar electrodes.

METHODS

Summary of experimental procedures

WE USED A bipolar RFA device (CelonPOWER System; OLYMPUS Winter & Ibe GmbH [Telto, Germany]) and two internally cooled bipolar electrodes (30-mm, 15-G, CelonProSurge; OLYMPUS Winter & Ibe GmbH). RFA was applied in the livers of three normal female domestic pigs (each pig's weight was 60 kg) under general anesthesia maintained until killing. The abdomen was opened so that the needle could be inserted under an ultrasonography (US) guide directly into the upper region of the liver where the thickness was larger than 3.5 cm. As a pig liver consists of five thin lobes, RFA sessions were performed two to three times in each liver for evaluation of the "no-touch pincer ablation procedure". After the experiments were completed, the animal was killed, and the ablated liver lobes were excised immediately. The specimen was cut in the plane of the needle tract and photographed to evaluate the shape and size of the ablated zone (white zone). The experimental protocol was approved by the Ethics Review Committee for Animal Experimentation of Toranomon Hospital.

Protocol of the no-touch pincer ablation procedure

We used a bipolar RFA device (CelonPOWER System; OLYMPUS Winter & Ibe GmbH), and all ablation procedures were performed with two internally cooled bipolar electrodes (30-mm, 15-G, CelonProSurge; OLYMPUS Winter & Ibe GmbH). Internal liquid circulation of the applicator enables the efficiency of coagulation to be increased. The delivery rate was set to 30 mL/min of saline solution at room temperature. The liquid flow was provided by a triple peristaltic pump, which is part of the system. The electrodes were operated by a power control unit working at 470 kHz and providing a maximum output power of 250 W (OLYMPUS Winter & Ibe GmbH). In this study, output power and total energy in each session were fixed at 60 W and 25 kJ, respectively, according to the dosimetry table for the bipolar RFA system (CelonPOWER System; OLYMPUS Winter & Ibe GmbH).

With regard to the ablation protocol, we performed the following three types of ablation procedure: linear insertion, at regular 13-mm intervals (pattern 1); fan-shape insertion, maximum interval of 20 mm (pattern 2); and 25 mm (pattern 3). All electrodes were inserted at a 30-mm depth from the liver surface under a US guide (Fig. 1). Each ablation procedure was performed for the following number of times: pattern 1, three sessions; pattern 2, three sessions; and pattern 3, two sessions. In this study, we assumed that the size of the virtual target tumor was less than 10 mm in pattern 1,

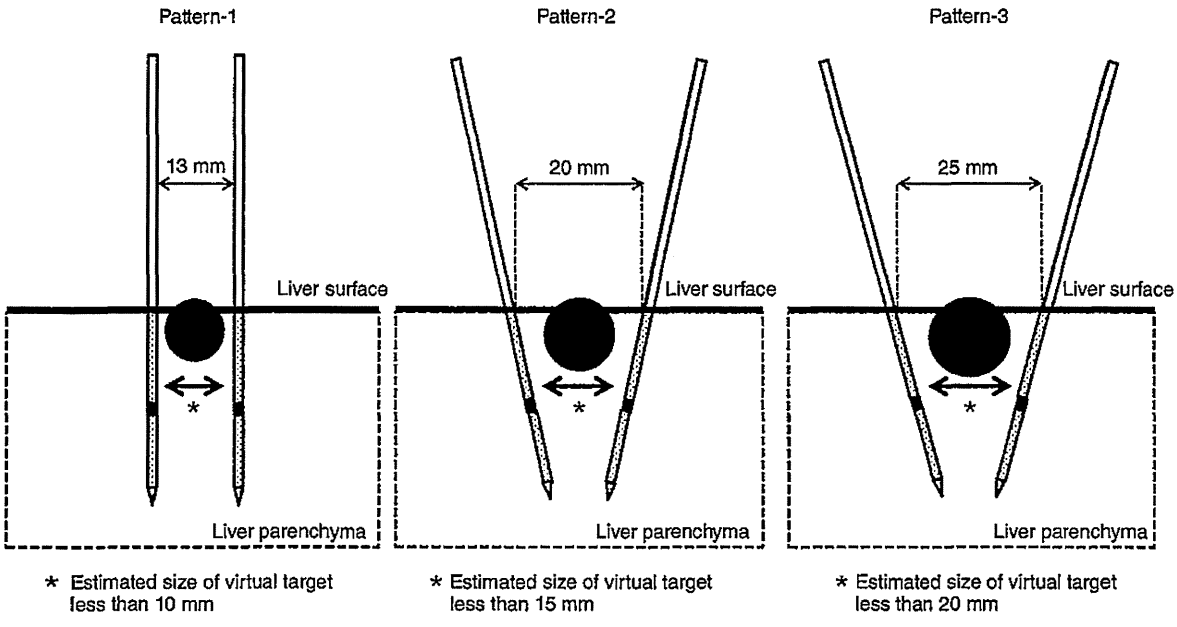

Figure 1 Protocol for a pincer ablation procedure that uses two internally cooled bipolar electrodes for a virtual nodule that protrudes from the liver surface.

less than 15 mm in pattern 2 and less than 20 mm in pattern 3.

Measurement procedure of the ablative margin

After completion of the experiments, the animal was killed and the ablated liver lobes were excised immediately. The specimen was cut in the plane of the needle tract and photographed to evaluate the shape and size of the ablated zone (white zone).

Statistical analysis

The size of the ablated zone and the duration of ablation were compared among the three groups with the Kruskal–Wallis test. All values are expressed as medians. A *P*-value of less than 0.05 denoted the presence of a statistically significant difference.

RESULTS

Features of the no-touch pincer ablation procedure

THE THREE TYPES of pincer ablation procedure applied to the pig liver were performed in the area shown in Figure 2(a).

Table 1 summarizes the features of each pincer ablation procedure for the treatment of the virtual target located on the liver surface.

In the median (range) transverse and longitudinal diameter to the shaft, ablative areas were: pattern 1, 32 (27–35) mm × 30 (30–35) mm; pattern 2, 27 (25–35) mm × 30 (30–32) mm; and pattern 3, 45 (40–50) × 26 (25–27) mm. There were no significant differences in the size of each ablative area among the three ablation procedures. However, with the pattern 3 procedure, the transverse diameter to the shaft was larger than with the other procedures, and as a result, the ablative form was flatter. On the other hand, patterns 1 and 2 acquired sufficient ablative areas that covered the liver surface with carbonization of the surface; however, with pattern 3, the ablative areas did not reach the liver surface, and carbonization of the liver surface was not apparent (Fig. 2b–d).

In addition, there were no significant differences among ablation procedures in the duration of ablative time.

DISCUSSION

WE OFTEN ENCOUNTER cases of HCC that are difficult to treat with RFA as a result of tumor location, especially nodules that protrude from the liver

(a)

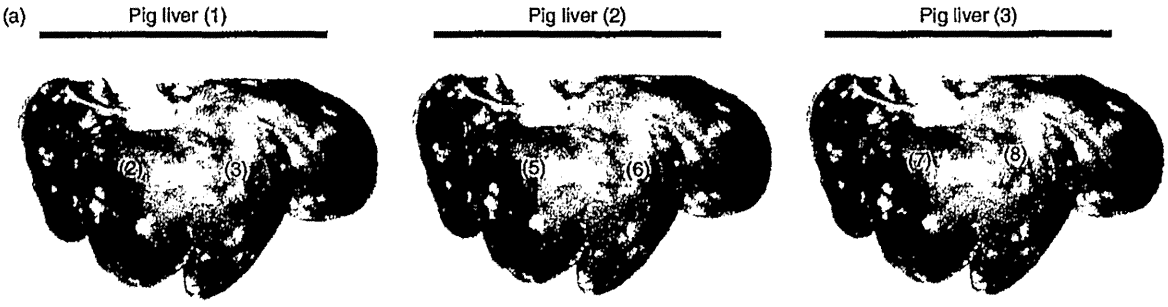

Ablative pattern	*Location*
Pattern-1: linear insertion, at regular 13-mm intervals	(1)(2)(5)
Pattern-2: fan-shape insertion, maximum interval, 20 mm	(3)(4)(7)
Pattern-3: fan-shape insertion, maximum interval, 25 mm	(6)(8)

(b) Representative ablative images: pattern-1

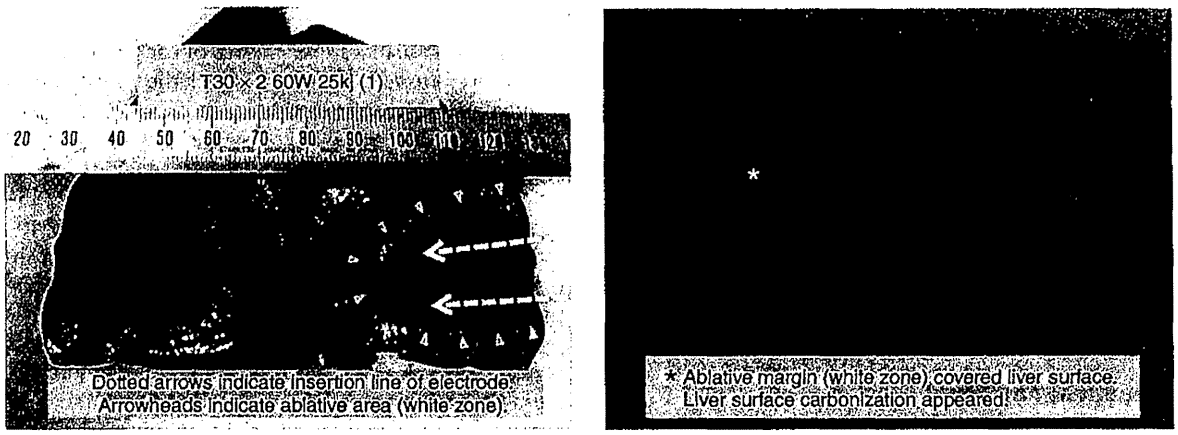

Figure 2 (a) Schema of the ablative areas of each pincer ablation procedure in the three pig livers. (b) One of the ablative shapes and the margin achieved with the pattern 1 procedure that uses two internally cooled bipolar electrodes for a virtual nodule that protrudes from the liver surface. With this pattern, we inserted the electrodes linearly (maximum interval for each electrode was 13 mm). The ablative margin covered the liver surface with carbonization of the liver surface. (c) One of the ablative shapes and the margin achieved with the pattern 2 procedure that uses two internally cooled bipolar electrodes for a virtual nodule that protrudes from the liver surface. With this pattern, we used a fan-shape insertion method (maximum interval for each electrode was 20 mm). The ablative margin covered the liver surface with carbonization of the liver surface. (d) Ablative shape and margin achieved with the Pattern 3 procedure that uses two internally cooled bipolar electrodes for a virtual nodule that protrudes from the liver surface. With this pattern, we used a fan-shape insertion method (maximum interval for each electrode was 25 mm). The ablative area close to the liver surface was larger than with the other procedures. However, the ablative margin did not cover the liver surface, and carbonization of the liver surface was not apparent.

(c) Representative ablative images: pattern-2

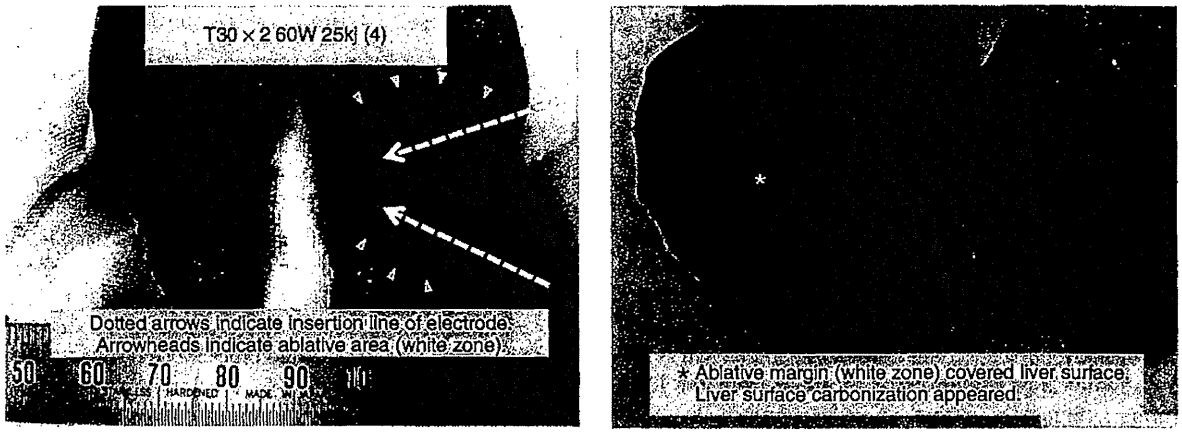

(d) Representative ablative images: pattern-3

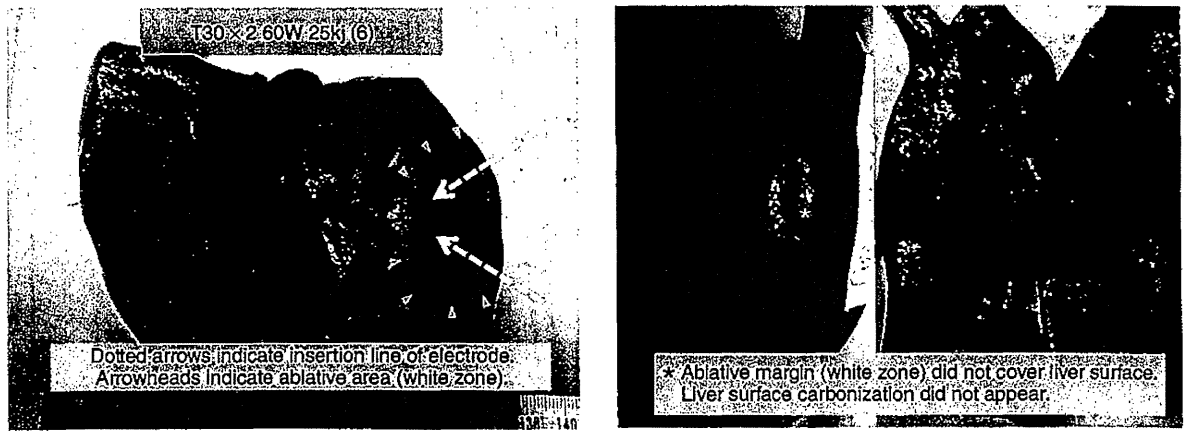

Figure 2 *Continued*

surface. In these situations, a multipolar ablation system that uses internally cooled bipolar electrodes may be suitable for treatment. With a multipolar ablation system, we can combine the use of one to three electrodes at the same treatment session, and when three electrodes are used, this system can treat a large tumor. However, in the case of small tumors (<20 mm), it is not really necessary to use three electrodes for treatment of the target tumor. However, in the dosimetry table of this bipolar system in Figure 3, which was made from previously reported early clinical data[16] and basic analysis, when two internally cooled bipolar electrodes are used (30 mm, 15-G, CelonProSurge; OLYMPUS Winter & Ibe GmbH), the recommended interval of each electrode in this system was 13 mm. With this regulation, we can treat only small tumors (<13 mm) when we perfume no-touch pincer ablation using two electrodes. Therefore, in this study we assumed a virtual target tumor with a tumor diameter less than 20 mm, and investigated the efficacy of a no-touch pincer ablation procedure and the maximum size of the tumor using two internally cooled bipolar electrodes for nodules that

Table 1 Features of each pincer ablation procedure for the treatment of the virtual target located on the liver surface

	Pattern 1			Pattern 2			Pattern 3		*P*
	1	2	3	1	2	3	1	2	
Duration	13′46″	13′16″	12′58″	14′38″	13′50″	13′30″	13′05″	12′40″	$P = 0.151$
Ablated area									
Transverse diameter, mm	27	35	32	25	27	35	45	40	$P = 0.113$
Longitudinal length, mm	35	30	30	32	30	30	27	25	$P = 0.102$
Ablated area covered liver surface	Yes	Yes	Yes	Yes	Yes	Yes	No	No	
Liver surface carbonization appeared	Yes	Yes	Yes	Yes	Yes	Yes	No	No	

protrude from the liver surface. In addition, we investigated only the fan-shape insertion method at a maximum interval of 20–25 mm. The reason for this is that in an actual RFA procedure, it is occasionally difficult to insert two electrodes in the same intercostal space for slightly large nodules that protrude from the liver surface; therefore, in this study, we examined a fan-shape ablation method that assumed two different intercostal approaches. Our results showed that with the pattern 3 treatment procedure, we could not acquire a sufficient ablative margin to the side of the liver surface. From these results, tumors of 20 mm or more may not be suitable for a no-touch pincer ablation procedure that uses two internally cooled bipolar electrodes in this bipolar system.

In contrast, with the pattern 1 and 2 treatment procedures, we acquired a sufficient ablative margin to the side of the liver surface with carbonization of the liver

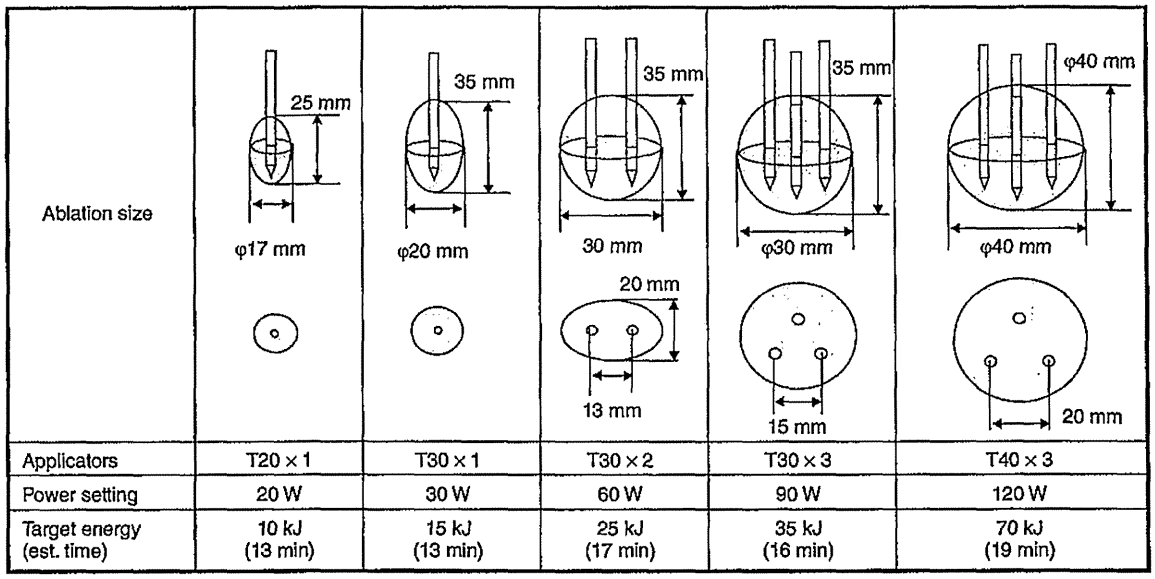

- The data are based on Frericks et al., Radiology (2005) 237: 1056–1062. The reported average efficacy was ~0.5 millitre ablation volume per kilojoule.
  From these data, the required energy for an ablation sphere or ellipsoid of given diameter was calculated.
- The application of blood flow interruption (e.g. Pringle's manoeuvre, embolization) allows for a significant reduction of the target energy.

Disclaimer: this dosimetry table does not replace the monitoring of actual ablation sizes. The ablation diameters are approximations based on statistical data; they are not guaranteed for individual clinical cases. Ablation size and shape as well as the procedure time may significantly vary due to tumor physiology and vascular structure. A deviation from the recommended applicator distances may also have an impact on the ablation dimensions.

Figure 3 Dosimetry table for the CelonPOWER system (in Japan).

surface. These results may indicate that tumors of less than 15 mm are candidates for the no-touch pincer ablation procedure that uses two internally cooled bipolar electrodes in this bipolar system.

Finally, this experimental animal study had some limitations. First, the number of animals was very small, and the target tumor was a virtual tumor. Second, an additional examination regarding a no-touch linear insertion procedure for maximum intervals of 20 mm and 25 mm for each electrode was not enforced. Third, we could not investigate the same fan-shape ablation procedure using monopolar RFA in this study, because we assumed it would be too difficult to carry out a two-step insertion method using a monopolar electrode under the influence of a first ablation for nodules that protrude from the liver surface. Fourth, we could not investigate the pathological changes in the ablative area in this study. Therefore, with only these study results, it may not be possible to draw conclusions regarding the utility of the fan-shape insertion method using a bipolar RFA device. To solve these problems, we must carry out an additional large-scale study that includes pathological examination in the near future.

Finally, to summarize the points to be noted at the time of performing the pincer ablation procedure, first, we should insert the needle carefully under US guidance, because in this procedure, measuring the distance of the needle tip from the liver surface and the two needle intervals on the liver surface correctly is the most important point.

Second, with this procedure, we should pay attention to the risk of thermal damage to the visceral peritoneum. Therefore, if possible, thermal protection using measures such as artificial ascites should be considered.

Third, in this study, we did not observe a portal or hepatic vein thrombus in the ablative area. However, this study was performed mainly in the vicinity of the liver surface, and usually this area does not include large vessels. Therefore, we need to use caution as with monopolar ablation when we ablate near large vessels.

In conclusion, the no-touch pincer ablation procedure (with an electrode interval of ≤20 mm) may be useful when performed with two internally cooled bipolar electrodes for small HCC tumors that protrude from the liver surface.

REFERENCES

1 Poon RT, Fan ST, Lo CM *et al.* Hepatocellular carcinoma in the elderly: results of surgical and nonsurgical management. *Am J Gastroenterol* 1999; 94: 2460–6.
2 Yamanaka N, Okamoto E, Toyosaka A *et al.* Prognostic factors after hepatectomy for hepatocellular carcinomas. A univariate and multivariate analysis. *Cancer* 1990; 65: 1104–10.
3 Kawasaki S, Makuuchi M, Miyagawa S *et al.* Results of hepatic resection for hepatocellular carcinoma. *World J Surg* 1995; 19: 31–4.
4 Shirabe K, Kanematsu T, Matsumata T, Adachi E, Akazawa K, Sugimachi K. Factors linked to early recurrence of small hepatocellular carcinoma after hepatectomy: univariate and multivariate analyses. *Hepatology* 1991; 14: 802–5.
5 Jwo SC, Chiu JH, Chau GY, Loong CC, Lui WY. Risk factors linked to tumor recurrence of human hepatocellular carcinoma after hepatic resection. *Hepatology* 1992; 16: 1367–71.
6 Nagasue N, Kohno H, Hayashi T *et al.* Lack of intratumoral heterogeneity in DNA ploidy pattern of hepatocellular carcinoma. *Gastroenterology* 1993; 105: 1449–54.
7 Izumi R, Shimizu K, Ii T *et al.* Prognostic factors of hepatocellular carcinoma in patients undergoing hepatic resection. *Gastroenterology* 1994; 106: 720–7.
8 Otto G, Heuschen U, Hofmann WJ, Krumm G, Hinz U, Herfarth C. Survival and recurrence after liver transplantation versus liver resection for hepatocellular carcinoma: a retrospective analysis. *Ann Surg* 1998; 227: 424–32.
9 Takayama T, Makuuchi M, Hirohashi S *et al.* Early hepatocellular carcinoma as an entity with a high rate of surgical cure. *Hepatology* 1998; 28: 1241–6.
10 Zhang BH, Yang BH, Tang ZY. Randomized controlled trial of screening for hepatocellular carcinoma. *J Cancer Res Clin Oncol* 2004; 130: 417–22.
11 Hong SN, Lee SY, Choi MS *et al.* Comparing the outcomes of radiofrequency ablation and surgery in patients with a single small hepatocellular carcinoma and well-preserved hepatic function. *J Clin Gastroenterol* 2005; 39: 247–52.
12 Stigliano R, Marelli L, Yu D, Davies N, Patch D, Burroughs AK. Seeding following percutaneous diagnostic and therapeutic approaches for hepatocellular carcinoma. What is the risk and the outcome? Seeding risk for percutaneous approach of HCC. *Cancer Treat Rev* 2007; 33: 437–47.
13 Kawamura Y, Ikeda K, Seko Y *et al.* Heterogeneous type 4 enhancement of hepatocellular carcinoma on dynamic CT is associated with tumor recurrence after radiofrequency ablation. *AJR Am J Roentgenol* 2011; 197: W665–W673.
14 Llovet JM, Vilana R, Brú C *et al.*, Barcelona Clínic Liver Cancer (BCLC) Group. Increased risk of tumor seeding after percutaneous radiofrequency ablation for single hepatocellular carcinoma. *Hepatology* 2001; 33: 1124–9.
15 Yu HC, Cheng JS, Lai KH *et al.* Factors for early tumor recurrence of single small hepatocellular carcinoma after percutaneous radiofrequency ablation therapy. *World J Gastroenterol* 2005; 11: 1439–44.
16 Frericks BB, Ritz JP, Roggan A, Wolf KJ, Albrecht T. Multipolar radiofrequency ablation of hepatic tumors: initial experience. *Radiology* 2005; 237: 1056–62.

Hepatology Research

Hepatology Research 2014; 44: E229–E239 doi: 10.1111/hepr.12254

Original Article

Hepatic oxidative stress in ovariectomized transgenic mice expressing the hepatitis C virus polyprotein is augmented through suppression of adenosine monophosphate-activated protein kinase/proliferator-activated receptor gamma co-activator 1 alpha signaling

Yasuyuki Tomiyama, Sohji Nishina, Yuichi Hara, Tomoya Kawase and Keisuke Hino

Department of Hepatology and Pancreatology, Kawasaki Medical School, Kurashiki, Japan

Aim: Oxidative stress plays an important role in hepatocarcinogenesis of hepatitis C virus (HCV)-related chronic liver diseases. Despite the evidence of an increased proportion of females among elderly patients with HCV-related hepatocellular carcinoma (HCC), it remains unknown whether HCV augments hepatic oxidative stress in postmenopausal women. The aim of this study was to determine whether oxidative stress was augmented in ovariectomized (OVX) transgenic mice expressing the HCV polyprotein and to investigate its underlying mechanisms.

Methods: OVX and sham-operated female transgenic mice expressing the HCV polyprotein and non-transgenic littermates were assessed for the production of reactive oxygen species (ROS), expression of inflammatory cytokines and antioxidant potential in the liver.

Results: Compared with OVX non-transgenic mice, OVX transgenic mice showed marked hepatic steatosis and ROS production without increased induction of inflammatory cytokines, but there was no increase in ROS-detoxifying enzymes such as superoxide dismutase 2 and glutathione peroxidase 1. In accordance with these results, OVX transgenic mice showed less activation of peroxisome proliferator-activated receptor-γ co-activator-1α (PGC-1α), which is required for the induction of ROS-detoxifying enzymes, and no activation of adenosine monophosphate-activated protein kinase-α (AMPKα), which regulates the activity of PGC-1α.

Conclusion: Our study demonstrated that hepatic oxidative stress was augmented in OVX transgenic mice expressing the HCV polyprotein by attenuation of antioxidant potential through inhibition of AMPK/PGC-1α signaling. These results may account in part for the mechanisms by which HCV-infected women are at high risk for HCC development when some period has passed after menopause.

Key words: antioxidant potential, glutathione peroxidase, reactive oxygen species, superoxide dismutase

INTRODUCTION

PERSISTENT HEPATITIS C virus (HCV) infection is a major risk factor for the development of hepatocellular carcinoma (HCC) in Japan. Approximately 70% of Japanese HCC patients are currently diagnosed with HCV-associated cirrhosis or chronic hepatitis C.[1] Nevertheless, the mechanisms underlying HCV-associated hepatocarcinogenesis are incompletely understood. Notably, there is sex disparity in HCC development, that is, male sex has been demonstrated to be an independent risk factor associated with HCC development.[2–4] It is proposed that estrogen-mediated inhibition of interleukin (IL)-6 production by Kupffer cells reduces the HCC risk in females.[5] In addition, the proportion of females among elderly patients with HCV-related HCC has recently increased in Japan.[6] These results suggest that menopause may be a risk factor associated with HCC development in female patients with HCV infection.

Numerous studies have shown that oxidative stress is present in chronic hepatitis C to a greater degree than in other inflammatory disease,[7,8] and is related to

Correspondence: Professor Keisuke Hino, Department of Hepatology and Pancreatology, Kawasaki Medical School, 577 Matsushima, Kurashiki, Okayama 701-0192, Japan. Email: khino@med.kawasaki-m.ac.jp

Received 9 September 2013; revision 24 September 2013; accepted 30 September 2013.

hepatocarcinogenesis in HCV-associated chronic liver diseases.[9,10] We have previously demonstrated that transgenic mice expressing the HCV polyprotein develop liver tumors including HCC, in connection with oxidative stress induced by HCV and iron overload.[11] Interestingly, such hepatocarcinogenesis was observed only in male transgenic mice, suggesting that females are resistant to oxidative stress in these transgenic mice. On the other hand, it is reported that ovariectomy increases nicotinamide adenine dinucleotide phosphate (NADPH) oxidase activity[12] and decreases mitochondrial-reduced glutathione levels in rats.[13] However, it remains unknown how HCV affects ovariectomy-induced oxidative stress. Investigation of this issue may provide a clue for understanding why the incidence of HCC increases in elderly postmenopausal women with HCV infection. The aim of this study was to determine whether HCV proteins amplify oxidative stress induced by ovariectomy and to investigate the mechanisms underlying this.

METHODS

Animals

CONTAINING THE FULL-LENGTH polyprotein-coding region under the control of the murine albumin promoter/enhancer, the transgene pAlbSVPA-HCV has been described in detail.[14,15] Of the four transgenic lineages with evidence of RNA transcription of the full-length HCV-N open reading frame (FL-N), the FL-N/35 lineage proved capable of breeding in large numbers. There is no inflammation in the transgenic liver.[15]

Experimental design

Female FL-N/35 transgenic mice and their normal female C57BL/6 littermates were anesthetized for surgery and underwent either a bilateral ovariectomy or sham operation at the age of 4–6 weeks. We studied ovariectomized (OVX) transgenic mice ($n = 5$), sham-operated transgenic mice ($n = 5$), OVX non-transgenic mice ($n = 5$) and sham-operated non-transgenic mice ($n = 5$). These mice were fed a normal rodent diet, bred, maintained, and killed by i.p. injection of 10% pentobarbital sodium preceded by 20-h fasting at the age of 24 weeks. All experimental protocols and animal maintenance procedures used in this study were approved by the Ethics Review Committee for Animal Experimentation of Kawasaki Medical School.

Histological procedures

A portion of liver tissue was immediately snap-frozen in liquid nitrogen for determination of the hepatic triglyceride concentration. The remaining liver tissue was fixed in 4% paraformaldehyde in phosphate-buffered saline and embedded in paraffin for histological analyses. Liver sections were stained with hematoxylin–eosin.

Serum leptin concentration

The serum leptin level was measured using a Rat Leptin Elisa kit (Morinaga Institute of Biological Science, Yokohama, Japan) according to the manufacturer's instructions.

Hepatic triglyceride content

Lipids were extracted from the homogenized liver tissue by the method of Bligh and Dyer.[16] The triglyceride level was measured with a TGE-test Wako kit (Wako Pure Chemicals, Tokyo, Japan), according to the manufacturer's instructions. Protein concentrations in liver were determined by the method of Lowry *et al.*,[17] using a DC protein assay kit (Bio-Rad Laboratories, Hercules, CA, USA).

In situ detection of reactive oxygen species (ROS)

In situ ROS production in the liver was assessed by staining with dihydroethidium, as described previously.[18] In the presence of ROS, dihydroethidium (Invitrogen, Carlsbad, CA, USA) is oxidized to ethidium bromide and stains nuclei bright red by intercalating with the DNA.[19] Fluorescence intensity was quantified using National Institutes of Health image analysis software for 3 randomly selected areas of digital images for each mouse.

Hepatic iron content

Hepatic iron content was measured by atomic absorption spectrometry, as described previously,[11] and expressed as micrograms Fe per gram of tissue (wet weight).

Derivatives of reactive oxygen metabolites (dROM) and biological antioxidant potential (BAP)

The levels of dROM and BAP were measured using a Free Radical Elective Evaluator (Wismerll, Tokyo, Japan), as described previously.[20] Measurement of dROM is based on the ability of the transition metal ions to catalyze the formation of alkoxy and peroxy radicals from hydroper-

oxides present in serum. The results are expressed in conventional units as Carrtelli units (U.CARR), where 1 U.CARR corresponds to 0.8 mg/L H_2O_2. Measurement of BAP is based on the ability of antioxidants to reduce ferric (Fe^{3+}) ions to ferrous (Fe^{2+}) ions.

RNA isolation and real-time reverse transcription polymerase chain reaction (RT–PCR)

Total RNA was isolated using an RNeasy mini kit (QIAGEN, Hilden, Germany) and reverse-transcribed into cDNA by using a Superscript III reverse transcription kit (Invitrogen). The PCR reactions were run in the ABI Prism 7700 sequence detection system (Applied Biosystems, Foster, CA, USA). The levels of mRNA were determined using cataloged primers (Applied Biosystems) for mice (tumor necrosis factor [TNF]-α, Mm00443258_m1; IL-1β, Mm00434228_m1; IL-6, Mm00446190_m1; HAMP [gene encoding hepcidin], Mm00519025_mL; superoxide dismutase 2 [SOD2], Mm01313000_m1; glutathione peroxidase 1 [GPx1], Mm00656767_g1; and sirtuin 3 [SIRT3], Mm00452131_m1). Expression of these genes was normalized to expression of glyceraldehyde 3-phosphate dehydrogenase mRNA (GAPDH, Mm99999915_g1).

Isolation of mitochondria and nuclear fraction

Mitochondrial extraction from liver tissue was performed using a Qproteome Mitochondrial Isolation kit (QIAGEN) according to the manufacturer's instructions. The nuclear fraction from liver tissue was prepared using a Nuclear Extraction kit (Panomics, Fremont, CA, USA) according to the manufacturer's instructions.

Immunoblotting

Liver lysates and the mitochondrial and nuclear fractions from liver were separated by sodium dodecylsulfate polyacrylamide gel electrophoresis. The proteins were transferred to polyvinylidene difluoride membranes (Millipore, Bradford, MA, USA), blocked overnight at 4°C with 5% skim milk and 0.1% Tween-20 in Tris-buffered saline, and subsequently incubated for 1 h at room temperature with goat antihuman SOD2 antibody (Santa Cruz Biotechnology, Santa Cruz, CA, USA), rabbit antihuman GPx1 antibody (Abcam, Cambridge, MA, USA), rabbit antihuman SIRT3 antibody (Abcam), rabbit antihuman peroxisome proliferator-activated receptor-γ co-activator-1α (PGC-1α) antibody (Abcam), rabbit antihuman adenosine monophosphate-activated protein kinase-α (AMPKα) antibody (Cell Signaling Technology, Boston, MA, USA), rabbit antihuman phospho-AMPKα (Thr172) antibody (Cell Signaling Technology), rabbit antihuman mitochondrial heat shock protein 70 antibody (HSP70; Thermo Scientific, Rockford, IL, USA), rabbit antihuman β-actin antibody (Cell Signaling Technology) or rabbit antimouse lamin B1 antibody (Abcam). The membranes were washed and incubated with horseradish peroxidase (HRP)-conjugated donkey antigoat immunoglobulin (Ig)G (Santa Cruz Biotechnology) or HRP-conjugated donkey antirabbit IgG (GE Healthcare Life Sciences, Pittsburgh, PA, USA).

Statistical analysis

Quantitative values are expressed as mean ± standard deviation. Two groups among multiple groups were compared by the rank-based Kruskal–Wallis ANOVA test followed by Scheffé's test. The statistical significance of correlation was determined by the use of simple regression analysis. $P < 0.05$ was considered to be significant.

RESULTS

Ovariectomy enhanced hepatic steatosis in FL-N/35 transgenic mice

As CONFIRMATION OF successful ovariectomy-induced suppression of endogenous estrogen production, the uterine weight of OVX mice was significantly decreased compared with that of sham-operated mice (Table 1). Dietary intake, bodyweight, liver weight and serum leptin levels were significantly greater in OVX mice than in sham-operated mice regardless of whether they were transgenic or non-transgenic (Table 1). Interestingly, the serum alanine aminotransferase (ALT) level was significantly higher in OVX transgenic mice than in mice in the other three groups, but the levels were comparable in OVX non-transgenic and sham-operated non-transgenic mice (Table 1). To determine why OVX transgenic mice have a higher ALT level, we investigated the liver histology of the mice in the four groups (OVX transgenic, sham-operated transgenic, OVX non-transgenic and sham-operated non-transgenic mice). In contrast to the mild to moderate degree of hepatic steatosis noted in OVX non-transgenic mice and sham-operated transgenic mice, OVX transgenic mice developed severe hepatic steatosis (Fig. 1a) without infiltration of inflammatory mononuclear cells. Hepatic triglyceride content was measured to quantify the degree of steatosis. The triglyceride content was significantly greater in OVX transgenic mice than in mice in the other three groups (Fig. 1b), which was consistent with the

Table 1 Body, liver and uterus weight and serum biochemical parameters

Body, liver, and uterus weight and serum biochemical parameters	Non-transgenic		Transgenic	
	Sham-operated	OVX	Sham-operated	OVX
Bodyweight (g)	21.5 ± 1.2	30.7 ± 4.9*	27.7 ± 4.6	34.2 ± 3.8**
Liver weight (g)	0.86 ± 0.075	1.09 ± 0.236*	0.90 ± 0.102	1.18 ± 0.156**
Ratio of liver to bodyweight	0.038 ± 0.037	0.035 ± 0.003	0.031 ± 0.002	0.034 ± 0.006
Uterus weight (g)	0.08 ± 0.01	0.01 ± 0.02*	0.09 ± 0.01	0.01 ± 0.01**
Total dietary intake (g)	337 ± 24	429 ± 13*	368 ± 28	490 ± 31**
Serum glucose (mg/dL)	222.9 ± 110.0	275.1 ± 121.4	284.0 ± 84.1	259.7 ± 108.9
Serum ALT (IU/L)	15.5 ± 6.5	30.6 ± 38.1	21.8 ± 11.4	281.2 ± 165.1***
Serum triglyceride (mg/dL)	99.9 ± 9.7	78.9 ± 10.8	98.3 ± 11.4	89.7 ± 13.3
Serum leptin (ng/mL)	0.45 ± 0.14	1.31 ± 0.31*	0.65 ± 0.22	1.60 ± 0.28**

Data are mean ± standard deviation.
*$P < 0.05$ compared with sham-operated non-transgenic mice. **$P < 0.05$ compared with sham-operated transgenic mice. ***$P < 0.01$ compared with mice in the other three groups.
ALT, alanine aminotransferase; OVX, ovariectomized.

results for hepatic steatosis. Thus, the increase in the serum ALT level in the OVX transgenic mice was thought to reflect the hepatic steatosis.

Ovariectomy increased ROS and IL-6 production in the liver

Only OVX transgenic mice showed marked hepatic steatosis, regardless of the comparable diet intake and the ratio of liver to bodyweight of OVX non-transgenic mice (Table 1). We have previously demonstrated that iron-overloaded male FL-N/35 transgenic mice expressing the HCV polyprotein develop severe hepatic steatosis through increased ROS production.[11] Therefore, we examined whether ROS production was relevant to the marked hepatic steatosis observed in the OVX transgenic mice. Ovariectomy significantly increased ROS (super-

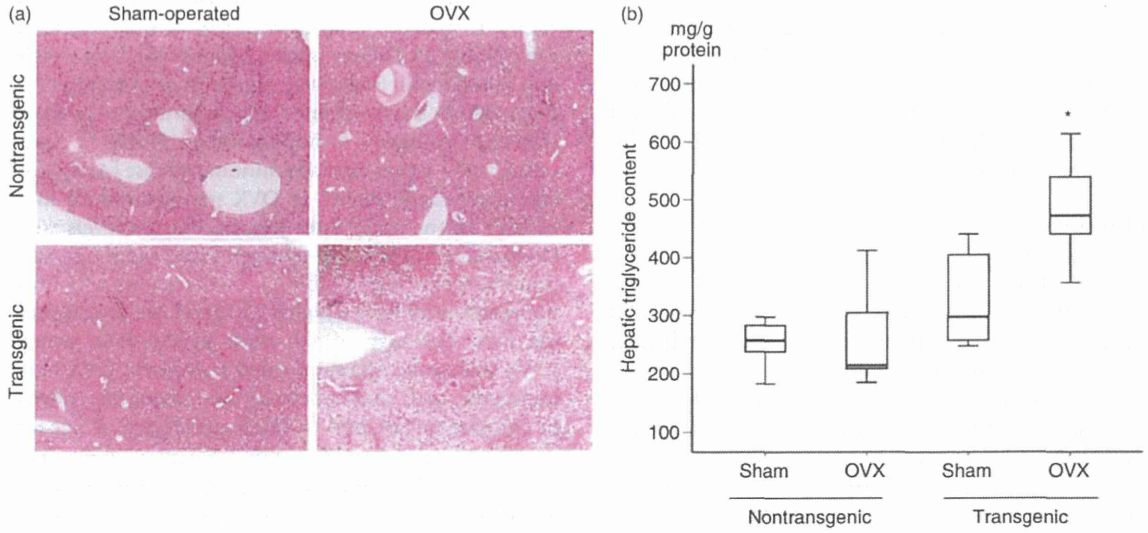

Figure 1 Hepatic steatosis and triglyceride content in sham-operated and ovariectomized (OVX) FL-N/35 transgenic and non-transgenic mice. (a) Hepatic steatosis in mice in each group (H&E, original magnification × 100). (b) Hepatic triglyceride content in mice in each group ($n = 5$). The results are shown as box plot profiles. The bottom and top edges of the boxes are the 25th and 75th percentiles, respectively. Median values are shown by the line within each box. *: $P < 0.05$ versus mice in the other three groups.

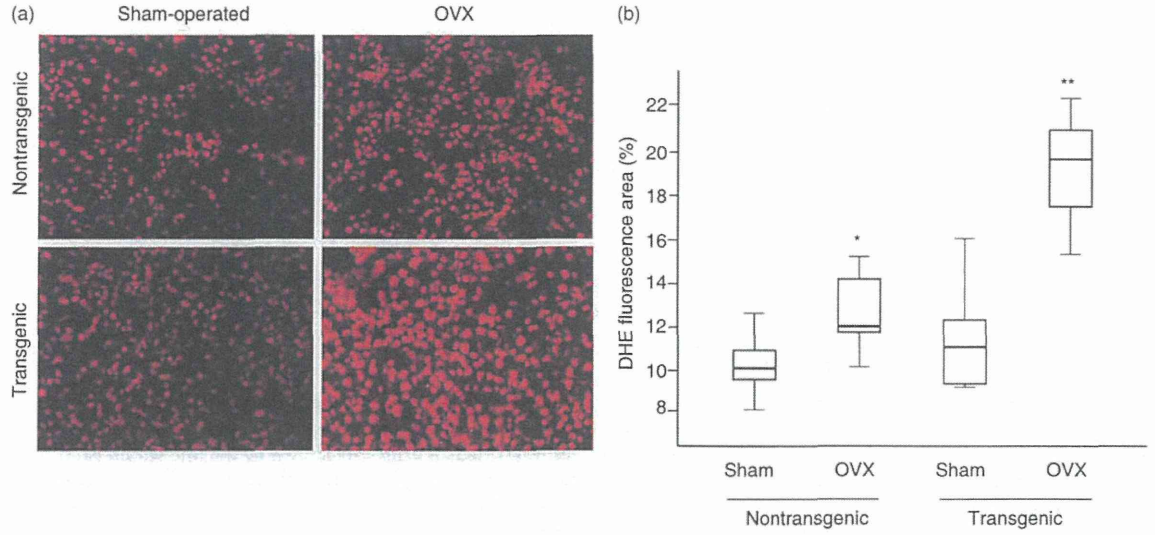

Figure 2 Reactive oxygen species (ROS) production in sham-operated and ovariectomized (OVX) FL-N/35 transgenic and non-transgenic mice. (a) Frozen liver sections from mice in each group were stained with dihydroethidium (DHE). (b) Fluorescence intensity was quantified by NIH image analysis software for three randomly selected areas of digital images for five mice in each group. The results are shown as box plot profiles. The bottom and top edges of the boxes are the 25th and 75th percentiles, respectively. Median values are shown by the line within each box. *: $P < 0.05$ versus sham-operated non-transgenic mice. **: $P < 0.05$ versus sham-operated nontransgenic mice, OVX non-transgenic mice and sham-operated transgenic mice.

oxide) production in both transgenic mice and non-transgenic mice, but the level of ROS production was greater in the OVX transgenic mice than in the OVX non-transgenic mice (Fig. 2). We next measured inflammatory cytokine levels in the liver. Ovariectomy significantly increased hepatic expression of IL-6 mRNA to the same degree in both transgenic mice and non-transgenic mice (Fig. 3). This ovariectomy-induced increase in hepatic IL-6 mRNA was consistent with the results of a previous report that OVX mice produced more hepatic

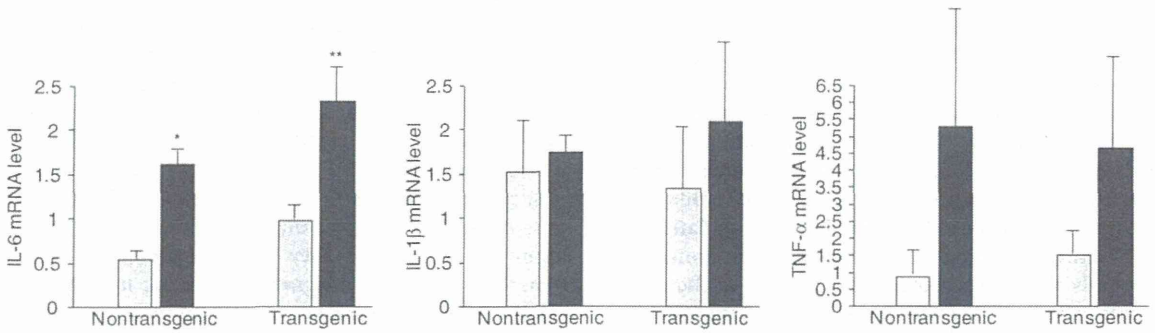

Figure 3 Expression levels of inflammatory cytokines in sham-operated and ovariectomized (OVX) FL-N/35 transgenic and non-transgenic mice. The mRNA levels of interleukin (IL)-6, IL-1β and tumor necrosis factor (TNF)-α were measured by real-time reverse transcription polymerase chain reaction for five mice in each group. The relative quantities of target mRNA in the liver were normalized with GAPDH mRNA. *$P < 0.05$ vs sham-operated non-transgenic mice. **$P < 0.05$ vs sham-operated transgenic mice. □, Sham; ■, OVX.

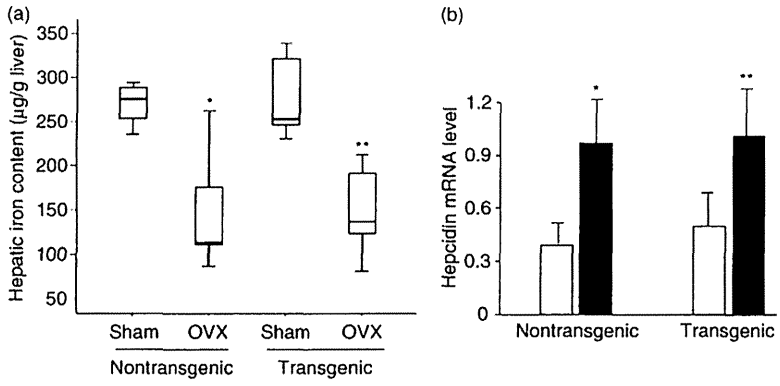

Figure 4 Hepatic iron content and hepcidin mRNA level in sham-operated and ovariectomized (OVX) FL-N/35 transgenic and non-transgenic mice. (a) Hepatic iron content in mice in each group ($n = 5$). The results are shown as box plot profiles. The bottom and top edges of the boxes are the 25th and 75th percentiles, respectively. Median values are shown by the line within each box. $^{*}P < 0.05$ vs sham-operated non-transgenic mice. $^{**}P < 0.05$ vs sham-operated transgenic mice. (b) The mRNA level of hepcidin was measured by real-time reverse transcription polymerase chain reaction for five mice in each group. The relative quantities of target mRNA in the liver were normalized with GAPDH mRNA. $^{*}P < 0.05$ vs sham-operated non-transgenic mice. $^{**}P < 0.05$ vs sham-operated transgenic mice. □, Sham; ■, OVX.

IL-6 than non-OVX mice after chemically induced liver injury.[5] There also was a trend for increase in TNF-α and IL-1β mRNA expression after ovariectomy in both the transgenic mice and non-transgenic mice, but their increases did not reach statistical significance, probably because of the large deviation (Fig. 3). These results suggested that inflammatory cytokines were unlikely to be associated with greater ROS production in OVX transgenic mice than in OVX non-transgenic mice.

Hepatic iron content and hepcidin expression level in the liver

We previously reported that male FL-N/35 transgenic mice developed hepatic iron accumulation through the reduced transcription of hepcidin,[18] a negative regulator in iron homeostasis.[21,22] Excess divalent iron can be highly toxic, mainly via the Fenton reaction producing hydroxyl radicals.[23] Therefore, we measured hepatic iron content to assess whether greater ROS production resulted from increased hepatic iron accumulation in OVX transgenic mice. Unexpectedly, ovariectomy significantly decreased hepatic iron content to the same degree in both transgenic mice and non-transgenic mice (Fig. 4a). These results are potentially explained by significantly increased transcription of hepcidin after ovariectomy (Fig. 4b). Ovariectomy-induced increase in hepatic IL-6 mRNA may in turn account for increased hepcidin transcription, because IL-6 acts to stimulate hepcidin expression through the STAT3 pathway.[24] These results suggested that hepatic iron content was not related to greater ROS production in OVX transgenic mice than in OVX non-transgenic mice.

Attenuated antioxidant potential against ovariectomy-induced ROS production in FL-N/35 transgenic mice

The increase in inflammatory cytokine production and the hepatic iron content after ovariectomy were comparable in transgenic and non-transgenic mice. Nevertheless, the serum ALT level, hepatic steatosis and ROS production were greater in OVX transgenic mice than in OVX non-transgenic mice. Therefore we measured dROM and BAP in serum to compare antioxidant potentials in OVX transgenic and OVX non-transgenic mice. We confirmed the significant negative correlation between the ratio of BAP to dROM and hepatic content of superoxide (Fig. 5). As expected, the values for dROM were higher in OVX mice than in sham-operated mice, regardless of whether they were transgenic or non-transgenic. However, a significant increase in the BAP value was found in OVX non-transgenic mice but not in OVX transgenic mice, which resulted in a lower ratio of BAP to dROM in the OVX transgenic mice than in the OVX non-transgenic mice (Table 2).

The first line of defense against ROS is the detoxifying enzymes that scavenge ROS. These include SOD and

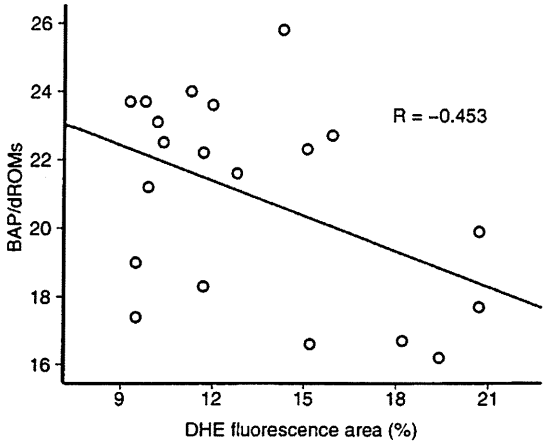

Figure 5 Negative correlation between the ratio of biological antioxidant potential (BAP) to derivatives of reactive oxygen metabolites (dROM) and hepatic content of superoxide. $R = -0.453$, $P < 0.05$. Hepatic content of superoxide was determined based on the area of dihydroethidium (DHE) fluorescence.

GPx1. Therefore we next investigated the expression levels of SOD2 and GPx1. The hepatic expression levels of SOD2 mRNA and GPx1 mRNA were significantly greater in OVX non-transgenic mice than in sham-operated non-transgenic mice, but were comparable in OVX transgenic mice and sham-operated transgenic mice (Fig. 6a). Western blot analysis of the hepatic mitochondria fractions also showed significant increases of SOD2 and GPx1 expression in OVX non-transgenic mice but not in OVX transgenic mice (Fig. 6b). These results suggested that antioxidant defense mechanisms may be induced against ovariectomy-related ROS production in non-transgenic mice but not in transgenic mice.

SIRT3 and PGC-1α expression in OVX FL-N/35 transgenic mice

Proliferator-activated receptor-γ co-activator-1α is a master regulator of mitochondrial biogenesis and respiration[25] and required for the induction of many ROS-detoxifying enzymes, including SOD2 and GPx1 upon oxidative stress.[26] SIRT3 is a member of a class III histone deacetylase and is reported to mediate PGC-1α-dependent induction of ROS-detoxifying enzymes.[27] In accordance with the changes in SOD2 and GPx1 levels after ovariectomy, the hepatic expression of SIRT3 mRNA was significantly greater in OVX non-transgenic mice than in sham-operated non-transgenic mice, but comparable in OVX transgenic mice and sham-operated transgenic mice (Fig. 7a). Western blot analysis of hepatic mitochondria showed a significant increase of SIRT3 expression in OVX non-transgenic mice but not in OVX transgenic mice (Fig. 7a).

Proliferator-activated receptor-γ co-activator-1α interacts with various nuclear receptors in addition to peroxisome proliferator-activated receptor-γ and is docked to the promoter of its target genes by all these nuclear receptors. Therefore, we investigated PGC-1α expression levels not only in liver homogenates but also in the nuclear fraction of mouse liver. The expression levels of PGC-1α in liver homogenates were comparable in sham-operated and OVX non-transgenic mice and in sham-operated and OVX transgenic mice. However, the expression levels of PGC-1α in the nuclear fraction of the liver significantly increased after ovariectomy in both non-transgenic and transgenic mice, and OVX transgenic mice had a lower PGC-1α expression level than OVX non-transgenic mice (Fig. 7b). These results suggested that the antioxidant potential against ovariectomy-induced ROS production may be reduced in OVX transgenic mice through lesser activation of PGC-1α than in OVX non-transgenic mice.

Table 2 Derivatives of reactive oxygen metabolites (dROM), biological antioxidant potential (BAP) and ratio of BAP to dROM

	Non-transgenic		Transgenic	
	Sham-operated	OVX	Sham-operated	OVX
dROM (U.CARR)	145.2 ± 15.1	158.7 ± 15.9*	170.8 ± 10.4	199.3 ± 21.1**
BAP (μmol/L)	3217 ± 123	3644 ± 177*	3362 ± 178	3542 ± 140
Ratio of BAP to dROM	22.3 ± 2.3	23.1 ± 2.0	20.8 ± 1.8	17.8 ± 1.9***

Data are mean ± standard deviation.
*$P < 0.05$ compared with sham-operated non-transgenic mice. **$P < 0.05$ compared with sham-operated transgenic mice. ***$P < 0.05$ compared with ovariectomized (OVX) non-transgenic mice.

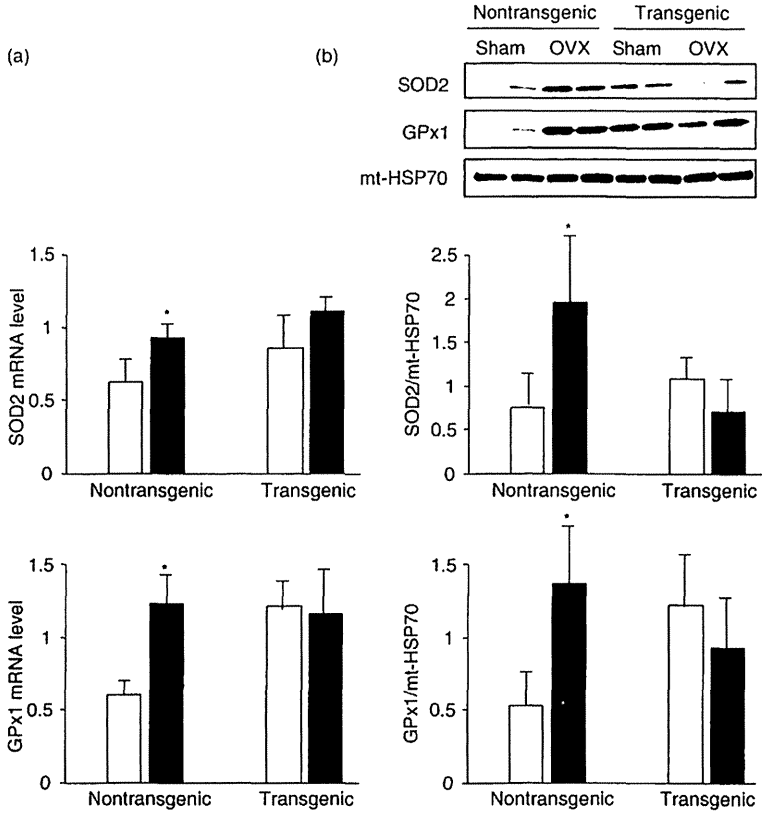

Figure 6 Expression levels of superoxide dismutase 2 (SOD2) and glutathione peroxidase 1 (GPx1) in sham-operated and ovariectomized (OVX) FL-N/35 transgenic and non-transgenic mice. (a) The mRNA levels of SOD2 and GPx1 were measured by real-time reverse transcription polymerase chain reaction for five mice in each group. The relative quantities of target mRNA in the liver were normalized with GAPDH mRNA. (b) Immunoblots for SOD2 and GPx1 were performed using mitochondrial fractions of liver lysates from five mice in each group. $^{*}P < 0.05$ vs sham-operated non-transgenic mice. □, Sham; ■, OVX.

Suppressed AMPK activation in OVX FL-N/35 transgenic mice

Proliferator-activated receptor-γ co-activator-1α activity is modulated through both transcriptional regulation and regulation of its activity by post-translational modifications.[28] AMPK is one of the signaling pathways regulating PGC-1α and acts both through modulation of PGC-1α transcription and by phosphorylation of the PGC-1α protein.[28] HCV has been shown to reduce the kinase activity of AMPK through Ser485/491 phosphorylation of AMPK.[29] Therefore, we examined the expression levels of AMPK to investigate the mechanisms underlying the lower PGC-1α expression in the nuclear fraction of the OVX transgenic liver. The expression levels of AMPKα, which is one of the three subunits (α, β and γ) of AMPK, were comparable in sham-operated and OVX mice and in non-transgenic and transgenic mice. However, the expression level of phosphorylated AMPKα was significantly greater in OVX non-transgenic mice than in mice in the three other groups, though it was similar in sham-operated transgenic mice and OVX transgenic mice (Fig. 7c). In addition, its levels were significantly greater in non-transgenic mice than in transgenic mice (Fig. 7c). These results suggested that AMPK was activated in OVX non-transgenic mice, but not in OVX transgenic mice, because AMPK is active only after phosphorylation of the α-subunit at a threonine residue within the kinase domain (T172) by upstream kinases.[30] Taken together, the results in the present study suggested that OVX FL-N/35 transgenic mice developed marked hepatic steatosis concomitant with increased ROS production via attenuation of antioxidant potential through inactivation of the AMPK/PGC-1α signaling pathway.

DISCUSSION

THE OVX MICE in the present study were assumed to be a standard model for evaluating the biological effect of ovariectomy because the effects of ovariectomy

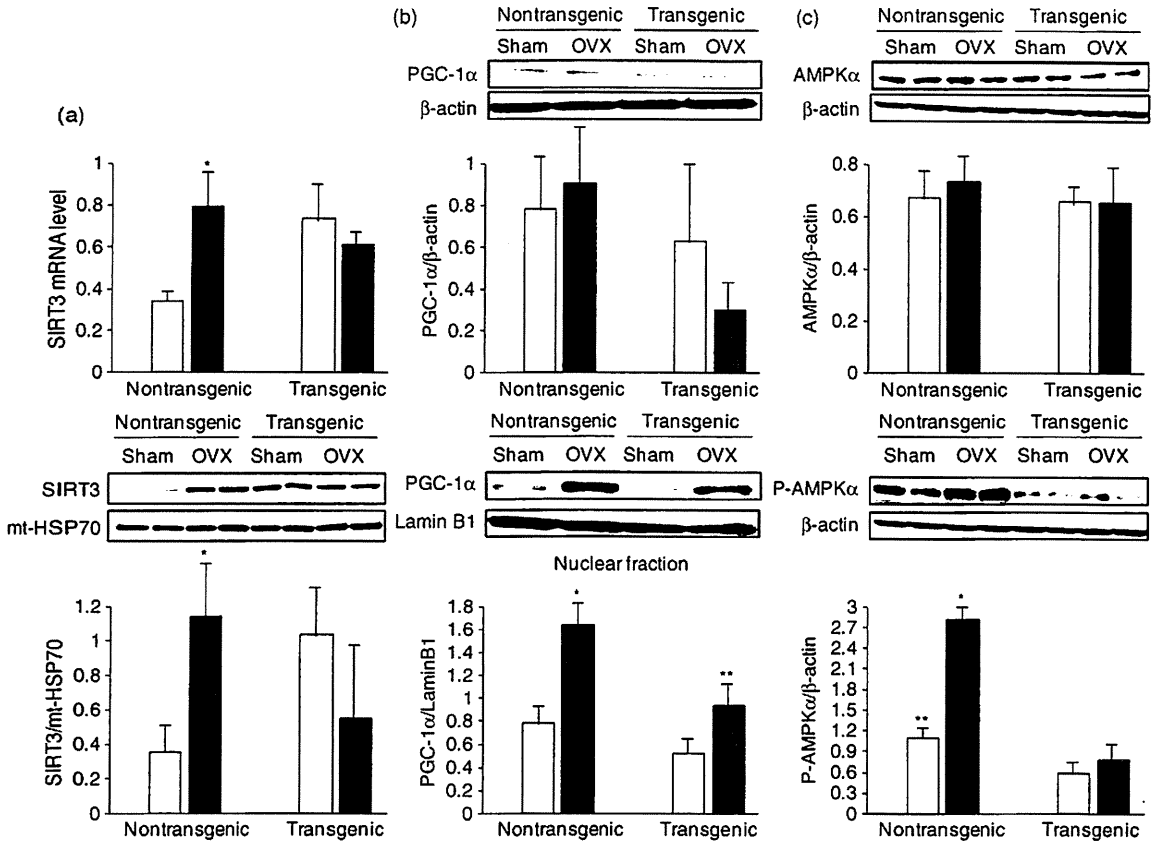

Figure 7 Expression levels of sirtuin 3 (SIRT3), peroxisome proliferator-activated receptor-γ co-activator-1α (PGC-1α), adenosine monophosphate-activated protein kinase α (AMPKα), and phosphorylated AMPKα (P-AMPKα) in sham-operated and ovariectomized (OVX) FL-N/35 transgenic and non-transgenic mice. (a) The mRNA levels of SIRT3 were measured by real-time reverse transcription polymerase chain reaction for five mice in each group. The relative quantities of target mRNA in the liver were normalized with GAPDH mRNA. Immunoblots for SIRT3 were performed using the mitochondrial fractions of liver lysates from five mice in each group. (b) Immunoblots for PGC-1α were performed using liver lysates and their nuclear fractions from five mice in each group. $^{*}P < 0.05$ vs mice in the other three groups. $^{**}P < 0.05$ vs sham-operated transgenic mice. (c) Immunoblots for AMPKα and P-AMPKα were performed using liver lysates from five mice in each group. $^{*}P < 0.05$ vs mice in the other three groups. $^{**}P < 0.05$ vs sham-operated transgenic mice. □, Sham; ■, OVX.

on dietary intake, bodyweight, uterine weight, liver weight and serum leptin levels were similar to the results from previous studies.[11–14] Ovariectomy increased ROS (superoxide) production in both transgenic liver and in non-transgenic liver, which was consistent with the ovariectomy-induced increase in NADPH oxidase activity[12] and the protective effect of estrogen against mitochondrial oxidative damage[13] found in previous studies. Of note was the much greater degree of ROS production after ovariectomy in transgenic mice than in non-transgenic mice. These results suggested that HCV protein expression has the potential to increase the sensitivity to oxidative stress in the liver. At least two possibilities may account for the increased sensitivity to oxidative stress in FL-N/35 transgenic mice. One possibility is an additive effect of HCV-induced ROS production on ovariectomy-induced oxidative stress. The HCV core protein has been shown to inhibit mitochondrial electron transport[15] and to induce ROS production.[16] In fact, basal ROS production tended to be higher in

transgenic mice than in non-transgenic mice, but was not significantly different. These results suggested that additive HCV-induced ROS production was unlikely to be the cause of the significantly increased ROS production after ovariectomy in the transgenic mice. The other possibility is HCV-associated attenuation of antioxidant potential against ovariectomy-induced oxidative stress. In this respect, OVX transgenic mice had a lower ratio of BAP to dROM than OVX non-transgenic mice and the expression of SOD2 and GPx1 in the liver was not increased. These results suggest that HCV protein attenuated antioxidant potential against ovariectomy-induced oxidative stress.

Proliferator-activated receptor-γ co-activator-1α is required for the induction of many ROS-detoxifying enzymes upon oxidative stress.[26] SIRT3 has been shown to function as a downstream target gene of PGC-1α and mediate the PGC-1α-dependent induction of ROS-detoxifying enzymes.[27] Additionally, AMPK, which is a crucial cellular energy sensor, regulates PGC-1α activity through both modulation of PGC-1α transcription and phosphorylation of the PGC-1α protein.[28,17] Thus, AMPK/PGC-1α signaling is one of the important pathways that protect cells from oxidative stress through the induction of several key ROS-detoxifying enzymes. Recent evidence indicating that HCV replication inhibits AMPK activity[29] prompted us to investigate whether the antioxidant potential against ovariectomy-induced oxidative stress in FL-N/35 transgenic mice was attenuated through inhibition of this signaling pathway. As expected, upon ovariectomy, AMPK was activated in non-transgenic mice, but not in transgenic mice. This, in turn, led to the lower expression of PGC-1α in the nuclear fraction of the liver in OVX transgenic mice than in OVX non-transgenic mice, resulting in the absence of significant induction of SIRT3 in the mitochondrial fraction of the liver in the OVX transgenic mice. Thus, ROS production in the liver in OVX transgenic mice was increased by attenuation of the antioxidant potential through inhibition of AMPK/PGC-1α signaling. However, it remains unknown why the expression of PGC-1α in the nuclear fraction was significantly increased in OVX transgenic mice regardless of the lack of activation of AMPK. Various kinases other than AMPK and post-translational modifications other than phosphorylation have been shown to regulate PGC-1α expression.[28] Therefore further investigations are required to clarify this issue.

Of particular concern is the relevance of the present results to HCC development in patients with HCV-associated chronic liver diseases. A recent study from Japan demonstrated a higher proportion of females, especially among elderly patients with HCV-related HCC, suggesting that the sex disparity in HCC development becomes less distinct as the patient's age at HCC diagnosis increases.[6] In general, ROS production creates a pro-carcinogenic environment under which chromosomal damage is likely to occur. The present findings that OVX transgenic mice have increased hepatic ROS production compared with that in OVX non-transgenic mice may indicate one of the mechanisms by which women with HCV infection are at high risk for HCC development when some period has passed after menopause, even though we need to clinically ascertain the increased hepatic oxidative stress in HCV-infected menopausal women with HCC.

ACKNOWLEDGMENTS

THIS RESEARCH WAS supported by a Grant-in-Aid for Scientific Research (B) (no. 23390201) and a Grant-in-aid for Exploratory Research (no. 25670374) from the Japan Society for the Promotion of Science, a Health and Labor Sciences Research Grant for Research on Hepatitis from the Ministry of Health, Labor and Welfare of Japan, and Research Project Grant P2 from Kawasaki Medical School.

REFERENCES

1 Chen DS, Locarnini S, Wait S *et al.* Report from a Viral Hepatitis Policy Forum on implementing the WHO framework for global action on viral hepatitis in North Asia. *J Hepatol* 2013. doi: 10.1016/j.jhep.2013.06.029.
2 Bruno S, Silini E, Crosignani A *et al.* Hepatitis C virus genotypes and risk of hepatocellular carcinoma in cirrhosis: a prospective study. *Hepatology* 1997; 25: 754–8.
3 Degos F, Christidis C, Ganne-Carrie N *et al.* Hepatitis C virus related cirrhosis: time to occurrence of hepatocellular carcinoma and death. *Gut* 2000; 47: 131–6.
4 Bosch FX, Ribes J, Diaz M, Cleries R. Primary liver cancer: worldwide incidence and trends. *Gastroenterology* 2004; 127: S5–S16.
5 Naugler WE, Sakurai T, Kim S *et al.* Gender disparity in liver cancer due to sex differences in MyD88-dependent IL-6 production. *Science* 2007; 317: 121–4.
6 Kumada T, Toyoda H, Kiriyama S *et al.* Characteristics of elderly hepatitis C virus-associated hepatocellular carcinoma patients. *J Gastroenterol Hepatol* 2013; 28: 357–64.
7 Farinati F, Cardin R, De Maria N *et al.* Iron storage, lipid peroxidation and glutathione turnover in chronic anti-HCV positive hepatitis. *J Hepatol* 1995; 22: 449–56.
8 Barbaro G, Di Lorenzo G, Asti A *et al.* Hepatocellular mitochondrial alterations in patients with chronic hepatitis C: